Radiation Physics and Chemistry 155 (2019) 9–16

Contents lists available at ScienceDirect

Radiation Physics and Chemistry

journal homepage: www.elsevier.com/locate/radphyschem

Estimation of conversion coefficients for absorbed and effective doses for pediatric CT examinations in two different PET/CT scanners

Ana P. Perini[a,b,c], William S. Santos[a,b], Lucio P. Neves[a,b], Walmir Belinato[d], Linda V.E. Caldas[c,*]

[a] Instituto de Física, Universidade Federal de Uberlândia, Av. João Naves de Ávila, 2121, 38400902 Uberlândia, MG, Brazil
[b] Programa de Pós-Graduação em Engenharia Biomédica, Faculdade de Engenharia Elétrica, Universidade Federal de Uberlândia, MG, Brazil
[c] Instituto de Pesquisas Energéticas e Nucleares, Comissão Nacional de Energia Nuclear (IPEN-CNEN/SP), Av. Prof. Lineu Prestes, 2242, 05508-000 SãoPaulo, SP, Brazil
[d] Departamento de Ensino, Instituto Federal de Educação, Ciência e Tecnologia da Bahia, Av. Amazonas 3150, 45030-220 Vitória da Conquista, BA, Brazil

ARTICLE INFO

Keywords:
Pediatric patients
Monte Carlo simulation
Computed tomography
Virtual anthropomorphic phantoms
Radiation doses

ABSTRACT

Normally, during medical procedures, special attention must be given to pediatric patients when compared to adults. This is specially relevant during procedures involving ionizing radiation, as CT scans, given that children are considerably more sensitive to radiation induced stochastic effects than adults. In order to investigate the radiation doses on radiosensitive organs of pediatric patients, undergoing head, chest and abdomen CT procedures, numerical dosimetry was employed in this work. The novelty is the use of a new set of pediatric virtual anthropomorphic phantoms, coupled with Monte Carlo simulation, to determine the conversion coefficients for absorbed and effective doses. Two CT equipment were simulated, taking into account the main characteristics of those commercially available. The results were converted to conversion coefficients (mGy/100 mA) for several organs and tissues, and the highest values were obtained for the newborn phantom. This numerical approach employed a new and reliable technique for pediatric CT dosimetry.

1. Introduction

Recently, pediatric patients undergoing computed tomography (CT) procedures presented a relevant increase. Several studies have been presented concerning dose evaluation in pediatric patients during CT scans (Al-Senan et al., 2012; Yang et al., 2014; Almohiy, 2014; Spampinato et al., 2015).

Three factors are very important in the dose evaluation of pediatric patients submitted to CT scans. First, in comparison with adult patients, children have a higher effective dose, given their body size differences (Brenner and Hall, 2007; Huda et al., 2001). Second, pediatric patients live longer than adults, resulting in a larger opportunity to develop a cancer, for example (Brenner and Hall, 2007). Third, untrained practitioners may use adult CT settings, during pediatric procedures, delivering radiation doses higher than necessary (Huda et al., 2001). Considering all these factors, the risk for pediatric stochastic effects is, inevitably, higher than that for adult patients. In this sense, radiation doses must be accurately calculated for pediatric patients, in an attempt to quantify these risks.

In recent decades, the use of Monte Carlo simulation for radiation dosimetry increased significantly. In order to determine the doses in different organs and tissues, which cannot be done experimentally, some virtual anthropomorphic phantoms were designed to be used together with Monte Carlo simulations. There are two types of virtual anthropomorphic phantoms more commonly utilized in radiation dosimetry: mathematical phantoms, or MIRD phantoms (Cristy, 1980), and computational phantoms based on voxels (de Melo Lima et al., 2011; Cassola et al., 2013).

Given the importance of dose evaluation in CT examinations to pediatric patients, the purpose of this study was to utilize pediatric virtual anthropomorphic phantoms and Monte Carlo simulation to determine the conversion coefficients (CC values) for organ doses and effective doses to newborn, 1-, 5-, and 10-year-old male and female phantoms.

This study adds to current understanding of the dose assessment by determining the CC values for absorbed and effective doses employing virtual phantoms, for different CT systems. To maintain a realistic representation of the organs and tissues, while keeping a lower computational time, the voxels that form the pediatric phantoms were resized to an edge of 0.24 cm long. This size is smaller than those from the literature, where normally larger voxel sizes are employed, limiting the precision on the contour of the organs. The results obtained in this work

* Corresponding author.
E-mail addresses: anapaula.perini@ufu.br (A.P. Perini), william@ufu.br (W.S. Santos), lucio.neves@ufu.br (L.P. Neves), wbfisica@gmail.com (W. Belinato), lcaldas@ipen.br (L.V.E. Caldas).

https://doi.org/10.1016/j.radphyschem.2018.07.009
Received 27 July 2017; Received in revised form 11 July 2018; Accepted 12 July 2018
Available online 30 July 2018

Table 1
Main characteristics of the pediatric virtual anthropomorphic phantoms used in this work de Melo Lima et al. (2011), Cassola et al. (2013).

Characteristics	Newborn	1y	5y		10y	
			F	M	F	M
Body mass (kg)	3.55	10.25	18.22	18.27	30.95	30.54
Height (m)	0.51	0.76	1.09	1.09	1.38	1.38
Body-Mass Index (kg/m^2)	13.91	17.73	15.30	15.34	16.23	16.01

Note: y stands for year, F for female and M for male.

Table 2
Main characteristics of the CT equipment used in this work.

PET/CT Scanner	Scan mode	Total beam collimation (mm)	Table increment (mm)	Pitch	Slice thickness (mm)
A	Helical	1.0 × 3.75	3.75	0.98 × 1 (0.98)	40 × 0.98 = 39.2
B	Helical	1.0 × 5.0	10.0	0.96 × 2 (1.92)	20 × 1.92 = 38.4

will allow a fast estimative of absorbed doses to organs, as well as effective doses, for pediatric patients of different ages, genders and CT scanner modes.

2. Materials and methods

2.1. Virtual anthropomorphic phantoms

In this work, pediatric phantoms were utilized, including a reference newborn, 1, 5-, and 10-year-old male and female phantoms, for radiation dosimetry calculations. These virtual phantoms were developed by the Radiation Dosimetry Group/Federal University of Pernambuco, Brazil. The characteristics of these phantoms are presented in Table 1, and more details of these virtual anthropomorphic phantoms can be found elsewhere (de Melo Lima et al., 2011; Cassola et al., 2013).

During a normal CT exam, the patients must keep their arms out of the radiation field. In order to maintain the simulations more realistic, the arms of the phantoms were also removed, except for the newborn and 1 year old patients. In these cases, as the patients are too young to be able to maintain their arms raised, it was decided to maintain the arms for a more realistic simulation. Therefore, there was a reduction on the mass of the skeleton bones and soft tissues. The modified bones include the clavicle, scapula and humerus. These structures have the potential to affect the absorbed doses to the organs, as lungs, esophagus, thymus and heart. Fig. 1 shows the front 3D views of the pediatric phantoms used in this work, with the examined regions (head, chest and abdomen).

2.2. Exposure scenarios

Two different exposure scenarios were modeled, employing two different CT scanners, named A and B, and several pediatric phantoms.

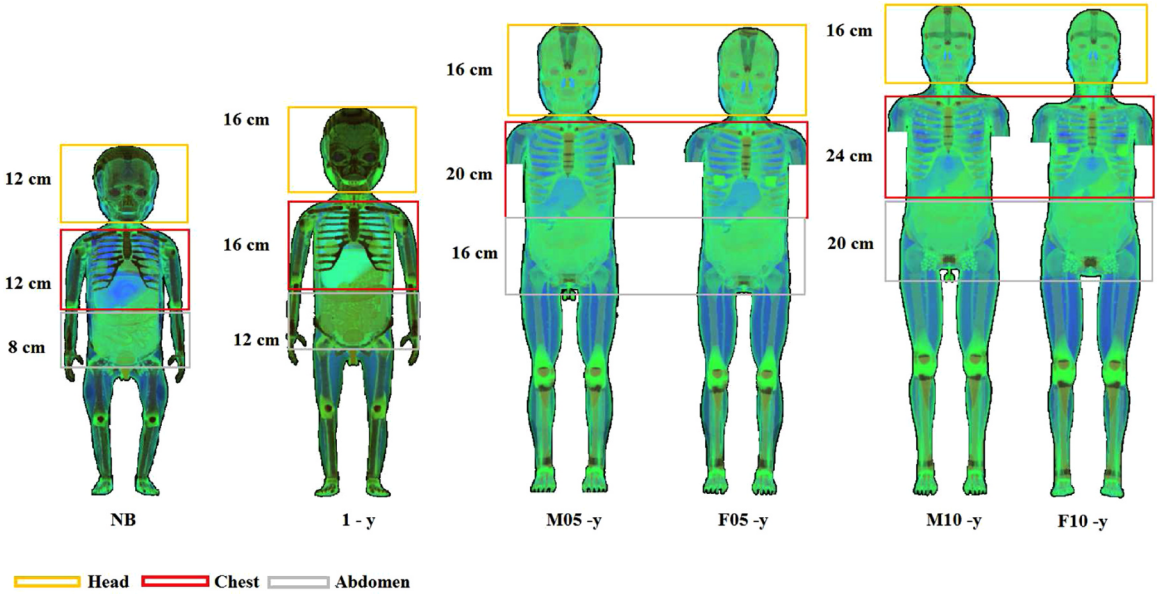

Fig. 1. Pediatric virtual anthropomorphic phantoms utilized in this work (Figure modified from de Melo Lima et al. (2011), Cassola et al. (2013)).

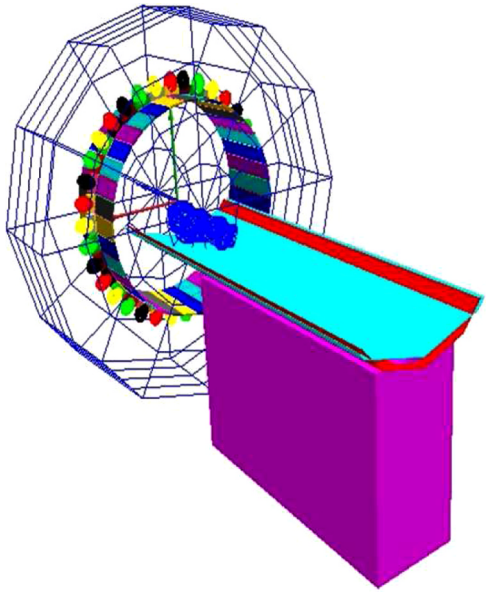

Fig. 2. Scenario of the Monte Carlo simulations composed by CT scanner and a pediatric virtual anthropomorphic phantom.

Equipment A allows the examination of the whole body with multidetector CT speed table of 40 mm/rot using 64-slice helical mode, and equipment B performs a whole body examination with multidetector CT speed table of 20 mm/rot in 16-slice helical mode. The tube voltages utilized for equipment A were: 80, 100, 120 and 140 kVp and, the tube voltages in equipment B were: 80, 110 and 130 kVp. These equipment were simulated for exams of variable helical pitch. A detailed description of the parameters is described in Table 2.

In order to reduce the patient doses, some modern CT scanners employ an automatic tube-current modulation (TCM). In this work, however, the TCM parameter has not been incorporated in the simulations, because Monte Carlo simulations are not able to simulate tube currents yet. All values obtained from these simulations were normalized by the number of photons emitted from the source. The reader must consider, however, that it did not affect the quality of these results, because the CC values were all normalized by the tube current-time product.

The technical specifications for the simulation of the CT scanners were obtained from the technical manual of the equipment and simulated within the general purpose of the Monte Carlo radiation transport code MCNPX (version 2.7.0) (Pelowitz, 2011). The CT scanner models validation was carried out by the comparison between experimental and simulated computed tomography dose index (CTDI). As presented in the literature (Belinato et al., 2015), the simulated and experimental results may reach an agreement up to 95%.

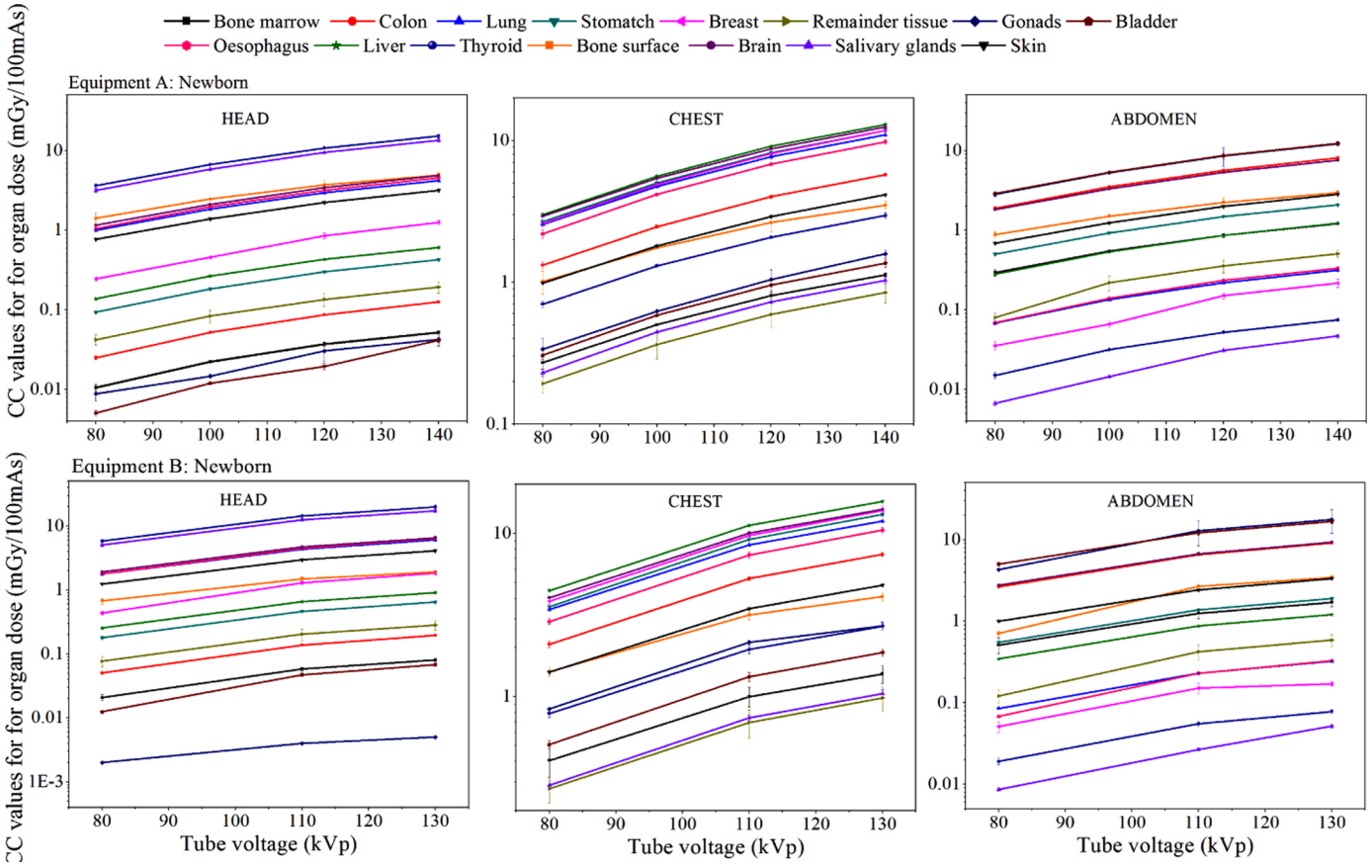

Fig. 3. CC values for organ doses (mGy/100 mAs) for the newborn phantom, as a function of the tube voltage of two equipment (A and B). Remainder tissues include: Adrenal, Gall Bladder, Heart, Kidneys, Lymphatic nodes, Muscle, Oral mucosa, Pancreas, Ovaries, Small intestine, Spleen, Thymus and Uterus. The gonads of man and woman were represented by the testicles and ovaries, respectively.

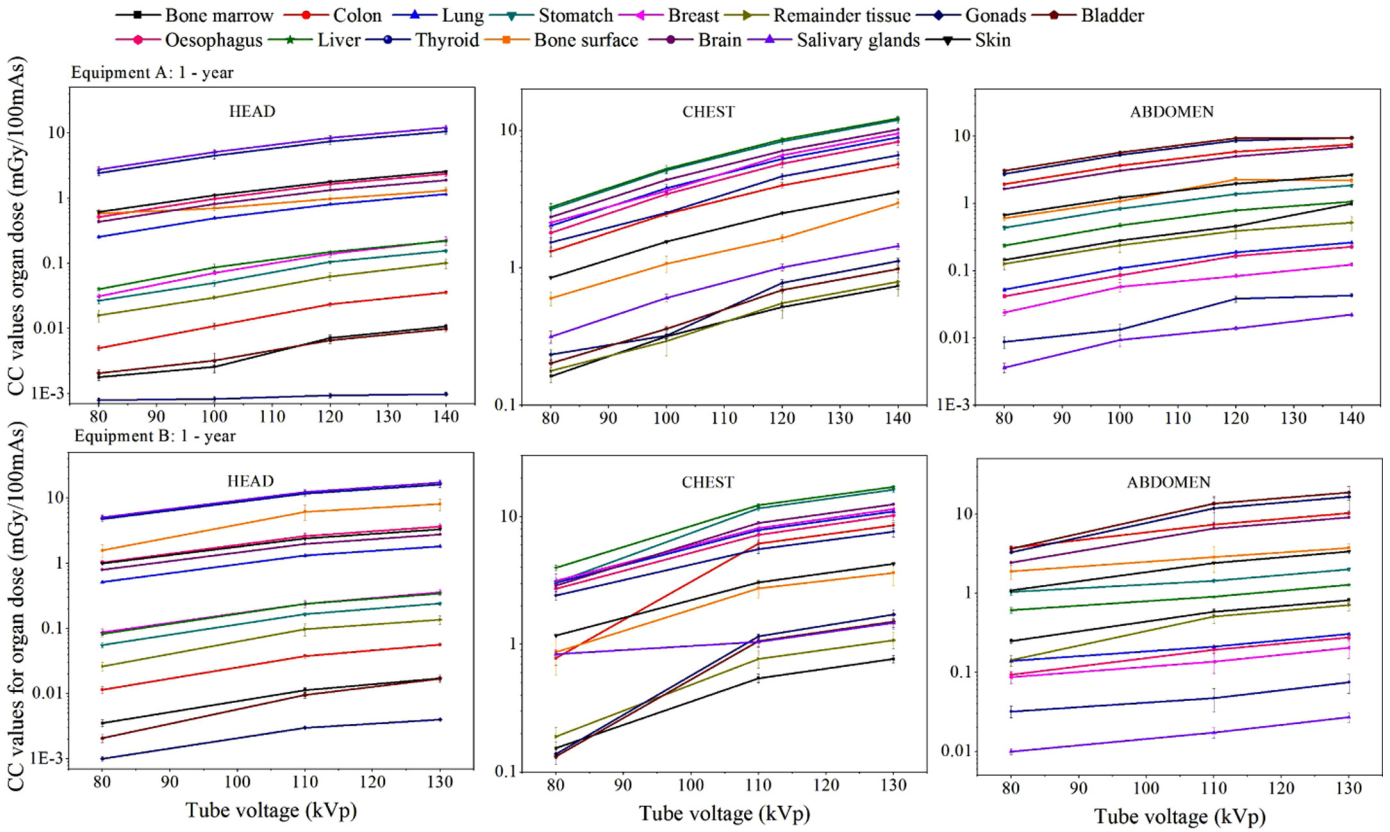

Fig. 4. CC values for organ doses (mGy/100 mAs) for the 1 year old phantom, as a function of the tube voltage of two equipment (A and B). Remainder tissues include: Adrenal, Gall Bladder, Heart, Kidneys, Lymphatic nodes, Muscle, Oral mucosa, Pancreas, Ovaries, Small intestine, Spleen, Thymus and Uterus. The gonads of man and woman were represented by the testicles and ovaries, respectively.

The X-ray source was modeled with a beam from a focal spot of 56° and a focal distance of 54 cm. The bowtie filter characteristics were also included. Its geometry was simulated through measurements of the total filtration at the center of the gantry, as already described by Belinato et al. (2015).

The X-ray spectrum of a CT scanner, utilized in this work, was generated by the SRS-78 software (Cranley et al., 1997). This software was chosen to be used in this study due to the possibility of filter combinations, which is very common among x-ray equipment. It generates energy spectra used in conventional radiology for tube voltages between 20 kVp and 150 kVp, for molybdenum, rhodium and tungsten targets. This software is one of the most used, and its accuracy has been extensively evaluated through comparisons with experimental results, which demonstrated that there is a small difference (less than 3%) between the measured and simulated half-value layer (Meyer et al., 2004).

The SRS-78 spectrum processing software allows the simulation of spectra for a variety of target and filter materials and thickness to be applied in the diagnostic radiology. This software employs a semi-empirical approach (Birch and Marshall model) (Cranley et al., 1997; Mohammadi et al., 2016), and uses the XCOM program to calculate the linear attenuation coefficients for different materials (Cranley et al., 1997).

The exposure scenario employed in this work, composed by a CT scanner and a pediatric virtual anthropomorphic phantom, is presented in Fig. 2.

2.3. Monte Carlo calculation of the conversion coefficients

A general purpose Monte Carlo transport code, MCNPX version 2.7.0 (Pelowitz, 2011), was utilized in this work for the simulations of the exposure scenarios. To incorporate the pediatric anthropomorphic phantoms into the MCNPX code, the dimensions of the voxels of the phantom were modified. To avoid memory allocation problems by the MCNPX code, arrays that represent the phantom were scaled so that the physiological and anatomical features were preserved. The resizing of arrays was performed through digital image processing software FANTOMAS (Vieira and Lima, 2009). Through this software, it was possible to increase the dimensions of the voxels from an edge of 0.12 cm to 0.24 cm, providing thus the incorporation of the phantom in the MCNPX code.

In order to determine the organ absolute doses, normalizing factors were used, relating the simulated dose values to experimental dosimetric quantities. The values employed in this work were presented elsewhere (Belinato et al., 2015). The effective doses were computed from the equivalent doses determined for the organs and tissues of the 5 and 10 year male and female phantoms, according to Eq. (1) (ICRP Publication 116, 2010).

$$E = \sum w_T \left[\frac{H_T^M + H_T^F}{2} \right] \quad (1)$$

where E is the effective dose, w_T is the dimensionless tissue-specific weighting factor and H_T^M and H_T^F are the tissue-specific equivalent doses in tissue T for a male (M) and a female (F) patients.

The CC values for organ absorbed doses, and effective doses were calculated using the *F6 tally* (MeV/g/particle) in MCNPX (10^9 initial particles were simulated).

3. Results and discussion

In this study a total of six pediatric anthropomorphic phantoms of

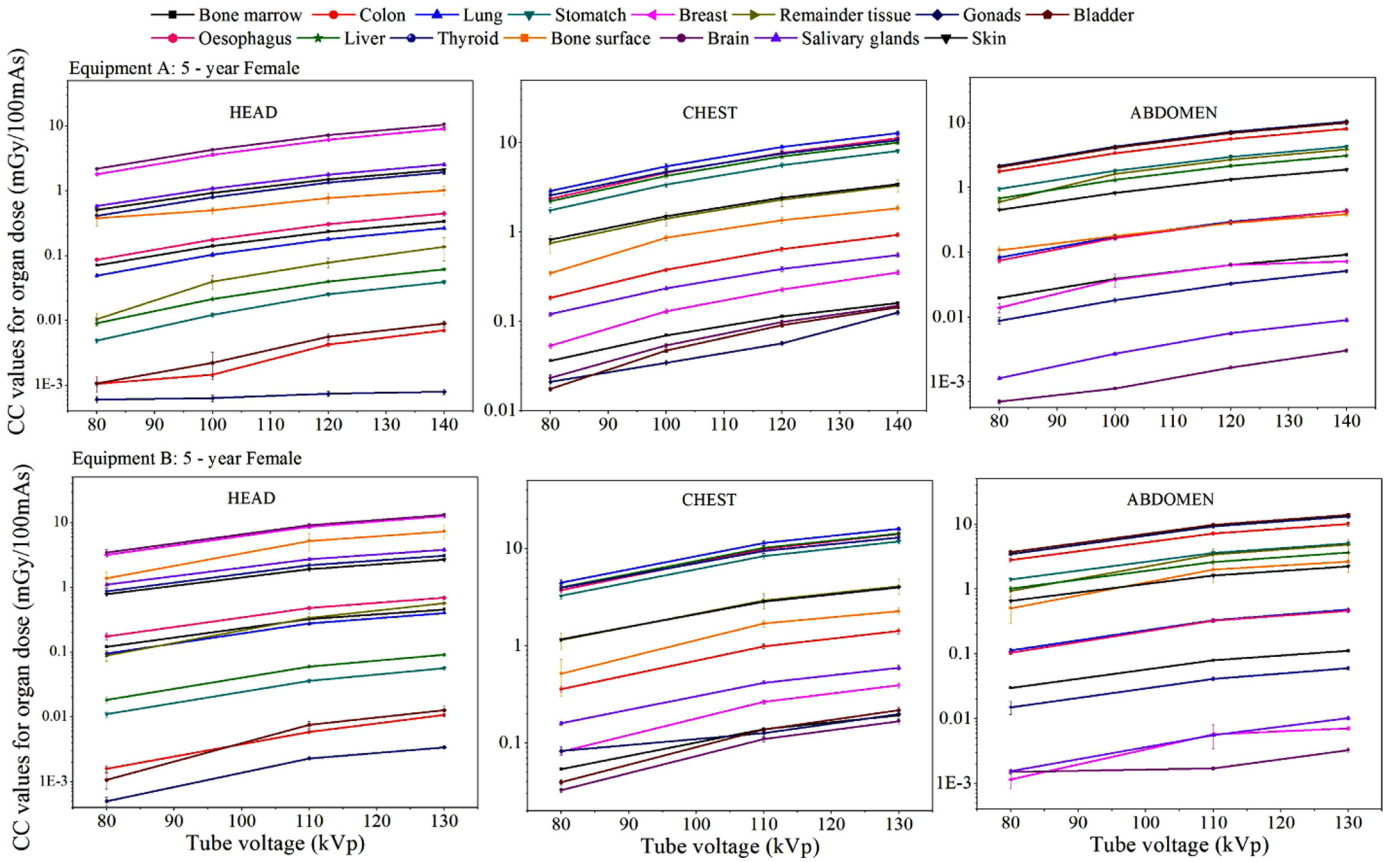

Fig. 5. CC values for organ doses (mGy/100 mAs) for the 5 year old female phantom, as a function of the tube voltage of two equipment (A and B). Remainder tissues include: Adrenal, Gall Bladder, Heart, Kidneys, Lymphatic nodes, Muscle, Oral mucosa, Pancreas, Ovaries, Small intestine, Spleen, Thymus and Uterus. The gonads of man and woman were represented by the testicles and ovaries, respectively.

different ages and sizes were utilized, coupled to the Monte Carlo method, allowing the assessment of the doses to organs and tissues of pediatric patients during different CT exams: head, chest and abdomen.

The influence of the tube voltage to the effective dose in the organs was evaluated. Furthermore, the differences in the absorbed doses to organs, caused by the anatomical differences among the virtual anthropomorphic phantoms, were also evaluated. The results showed significant differences between the two tested types of CT scanners.

The CC values for organ doses for newborn, 1-year old, 5-years old male, 5-years old female, 10-years old male and 10-years old female pediatric virtual phantoms are shown in Figs. 3 to 8, respectively. Even though no scan protocols employ 130 kVp and 140 kVp for newborn and 1 year old patients, they were used in order to warn clinical staff about the increase in CC values.

The CT equipment B presented higher CC values for all organs evaluated (Figs. 3–8). This is mainly due to the influence of the slice thickness, which is half of the equipment A. As a consequence, it takes a greater number of slices, increasing the doses of the patients. The influence of these differences on the image quality was not assessed in this work. Furthermore, as expected and demonstrated, an increase of the tube voltage resulted in higher CC values for organ doses, and consequently, for the CC values for effective doses. The CC values for effective doses were evaluated by gender; they decrease as the age increases.

The tube potential increase causes significant changes in the CC values for effective dose, as shown in Fig. 9. In general, regardless of the size of the phantoms, the equipment A operating with a 100 kVp tube voltage resulted in a CC for effective dose almost twice the value calculated for 80 kVp. The value for 120 kVp resulted in an increase of almost three times. The tube currents were kept constant. Similar results were obtained for the equipment B: 2.5 times (110–80 kVp) and 3.5 times (130–80 kVp).

According to results shown in Fig. 9 it is possible to observe that the highest CC values for effective dose were obtained for the newborn phantom. This can be explained by the fact that the photons may be less attenuated by the surrounding tissues in a small phantom, such as a newborn phantom. The smaller newborn organ masses are expected to result in much higher scattered radiation doses than for other phantoms, and therefore, the doses received by the organs and tissues of a newborn patient are high. For the other phantoms, there is a small difference among the CC values for effective dose.

4. Conclusion

In this work CC values for absorbed doses to organs, and effective doses, were evaluated for a new set of pediatric virtual anthropomorphic phantoms, submitted to head, chest and abdomen CT scans. Two different CT scanner configurations, with different tube voltages were also evaluated. A list of CC values were obtained for the main organs and tissues, providing a clear perspective of the dose involved in these exams. The main advantage of this work was to use detailed CT equipment, where all projections were carefully simulated, and a new set of virtual anthropomorphic phantoms, providing more reliable and realistic results. Besides that, this work provided CC values for organ doses and effective doses, utilizing two CT scanners and new pediatric virtual phantoms, showing, therefore, new results, since this type of information is not available in the literature. Moreover, it was possible to observe that the radiation doses to pediatric patients may depend on factors associated with the gender, size, tube voltage and CT equipment model.

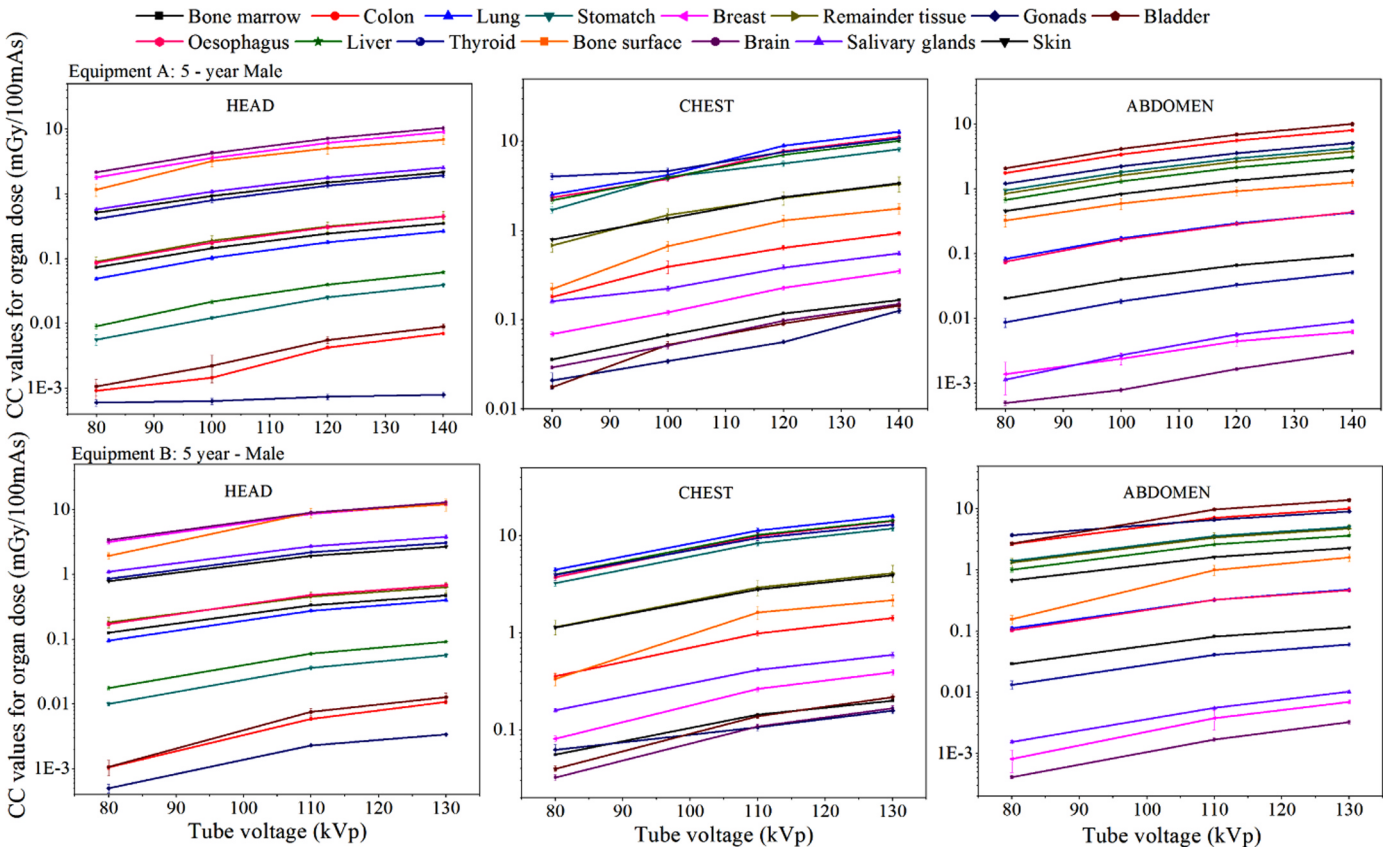

Fig. 6. CC values for organ doses (mGy/100 mAs) for the 5 year old male phantom, as a function of the tube voltage of two equipment (A and B). Remainder tissues include: Adrenal, Gall Bladder, Heart, Kidneys, Lymphatic nodes, Muscle, Oral mucosa, Pancreas, Small intestine, Spleen and Thymus. The gonads of man and woman were represented by the testicles and ovaries, respectively.

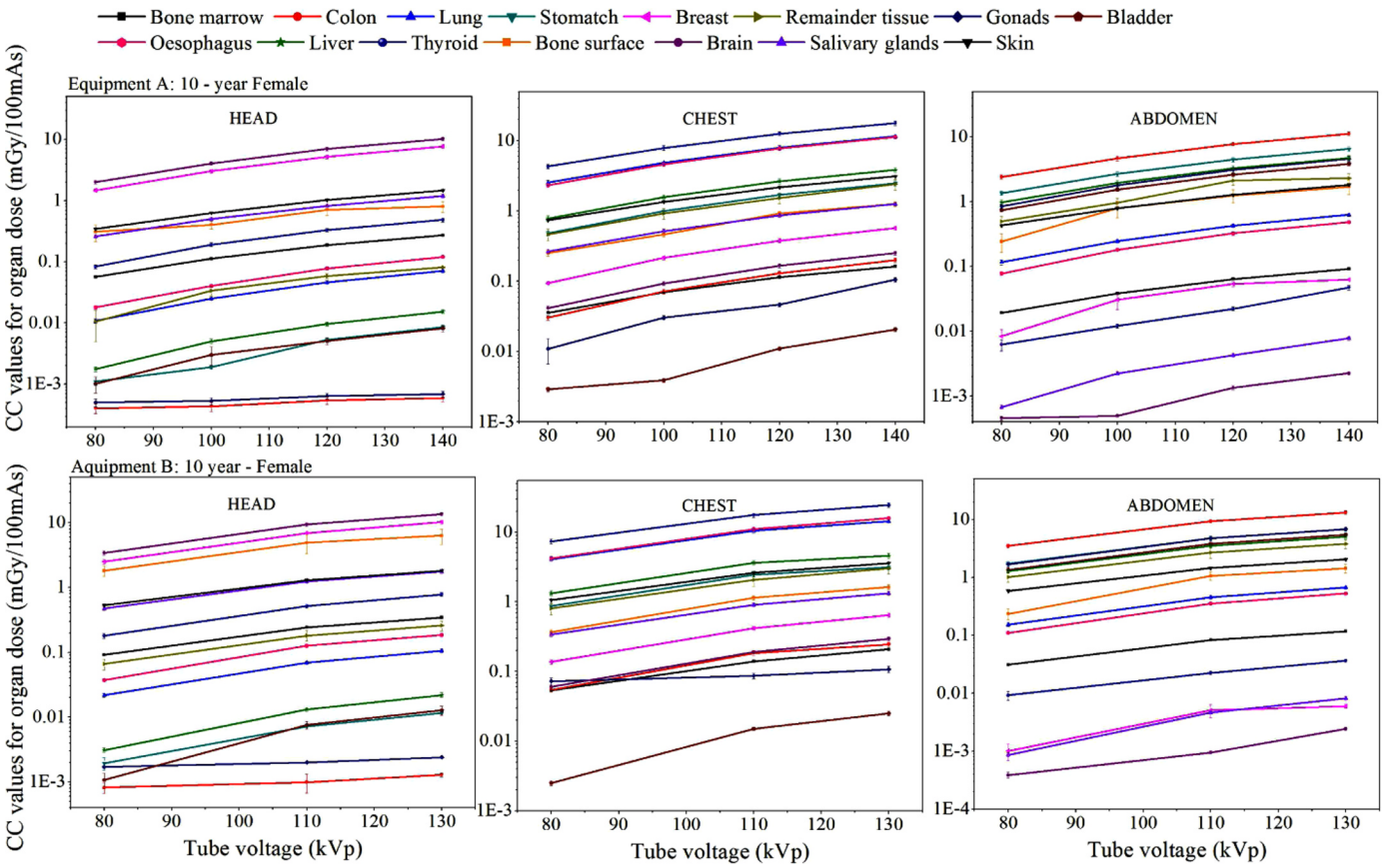

(caption on next page)

Fig. 7. CC values for organ doses (mGy/100 mAs) for the 10 year old female phantom, as a function of the tube voltage of two equipment (A and B). Remainder tissues include: Adrenal, Gall Bladder, Heart, Kidneys, Lymphatic nodes, Muscle, Oral mucosa, Pancreas, Ovaries, Small intestine, Spleen, Thymus and Uterus. The gonads of man and woman were represented by the testicles and ovaries, respectively.

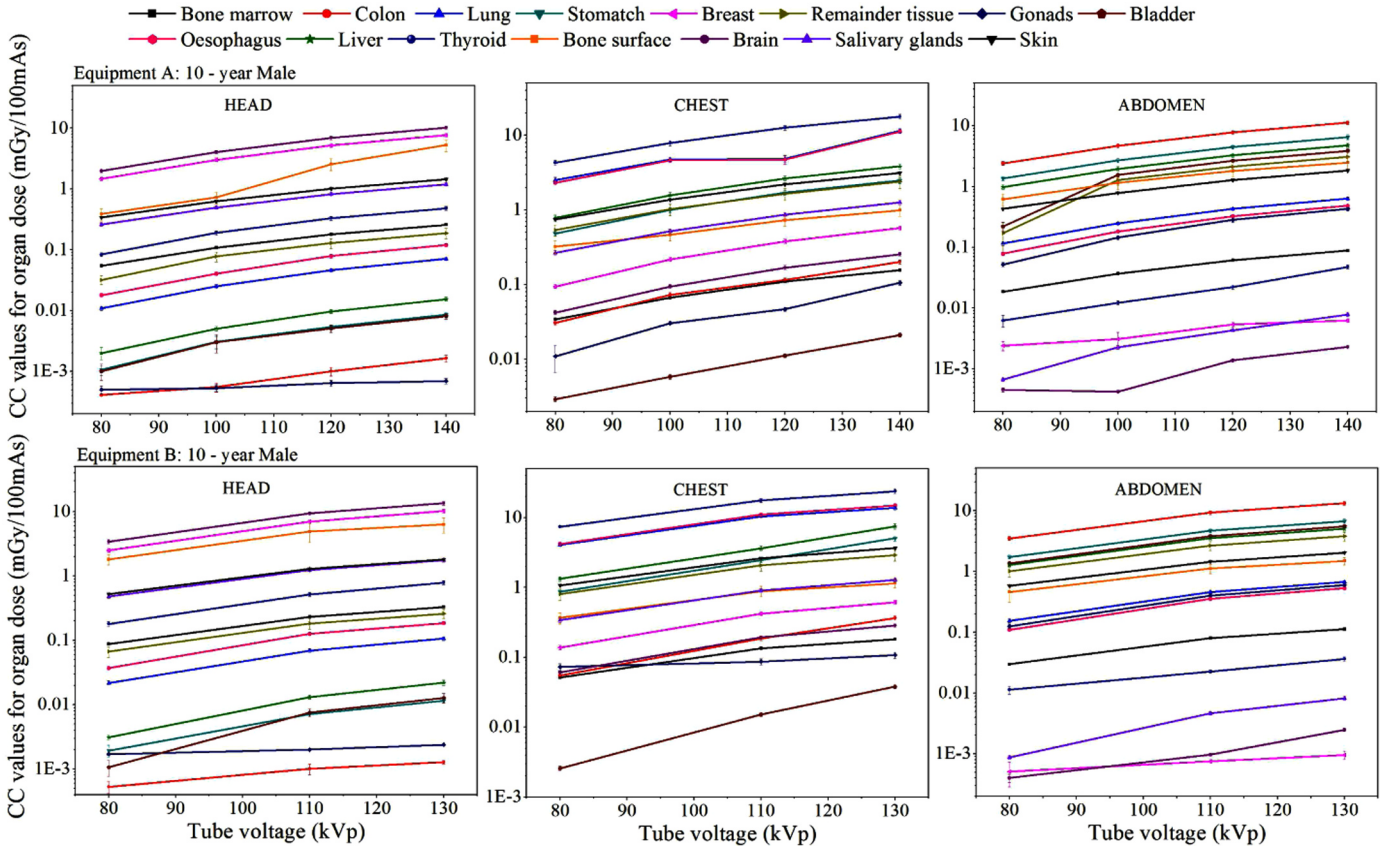

Fig. 8. CC values for organ doses (mGy/100 mAs) for the 10 year old male phantom, as a function of the tube voltage of two equipment (A and B). Remainder tissues include: Adrenal, Gall Bladder, Heart, Kidneys, Lymphatic nodes, Muscle, Oral mucosa, Pancreas, Small intestine, Spleen and Thymus. The gonads of man and woman were represented by the testicles and ovaries, respectively.

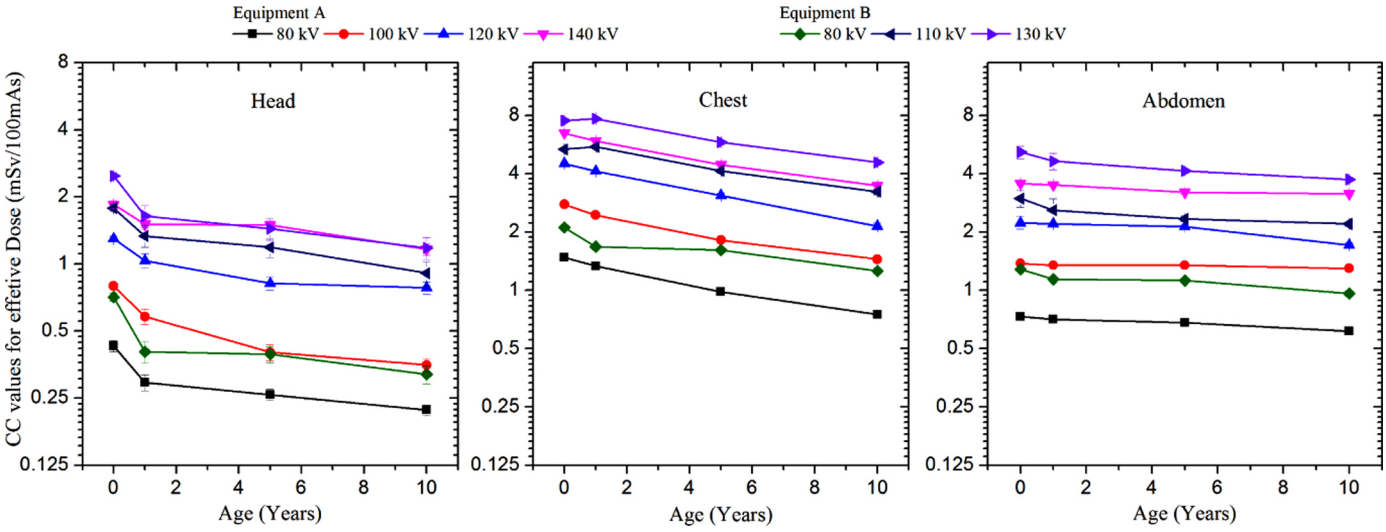

Fig. 9. CC values for effective doses (mSv/100 mAs) for the head, chest and abdomen, as a function of the age (years) for all pediatric phantoms evaluated in this work. The results are presented for different tube voltages, depending on the equipment employed.

Acknowledgments

The authors would like to thank Dr. Richard Kramer for kindly providing the virtual anthropomorphic phantoms. This work was partially supported by the Brazilian agencies: Fundação de Amparo à Pesquisa do Estado de Minas Gerais (FAPEMIG, Grants No. APQ-03049-15 and APQ-02934-15) and Conselho Nacional de Desenvolvimento Científico e Tecnológico (CNPq, Grants Nos. 421603/2016-0, 420699/2016-3, 168947/2017-0 and 301335/2016-8).

References

Almohiy, H., 2014. Paediatric computed tomography radiation dose: a review of the global dilemma. World J. Radiol. 6 (1), 1–6. https://doi.org/10.4329/wjr.v6.i1.1.

Al-Senan, R., Mueller, D., Hatab, M., 2012. Estimating thyroid dose in pediatric CT exams from surface dose measurement. Phys. Med. Biol. 57 (13), 4211–4221. https://doi.org/10.1088/0031-9155/57/13/4211.

Belinato, W., Santos, W.S., Paschoal, C.M.M., Souza, D.N., 2015. Monte Carlo simulations in multi-detector CT (MDCT) for two PETCT scanner models using MASH and FASH adult phantoms. Nucl. Instrum. Methods Phys. Res. Sect. A: Accel., Spectrometers, Detect. Assoc. Equip. 784 (1), 524–530. https://doi.org/10.1016/j.nima.2014.09.036.

Brenner, D.J., Hall, E.J., 2007. Computed tomography - an increasing source of radiation exposure. New Engl. J. Med. 357, 2277–2284. https://doi.org/10.1056/NEJMra072149.

Cassola, V.F., Kramer, R., de Melo Lima, V.J., de Oliveira Lira, C.A.B., Khoury, H.J., Vieira, J.W., Brown, K.R., 2013. Development of newborn and 1-year-old reference phantoms based on polygon mesh surfaces. J. Radiol. Prot. 33 (3), 669–691. https://doi.org/10.1088/0952-4746/33/3/669.

Cranley, K., Gilmore, B., Fogarty, G., Despond, L., 1997. Catalogue of diagnostic X-ray data and other data. Tech. Rep. 78. Institute of Physics and Engineering in Medicine (IPEM).

Cristy, M., 1980. Mathematical phantoms representing children of various ages for use in estimates of internal dose. Commission Rep. NUREG/CR-1159. U.S. Nuclear Regulatory.

de Melo Lima, V.J., Cassola, V.F., Kramer, R., de Oliveira Lira, C.A.B., Khoury, H.J., Vieira, J.W., 2011. Development of 5- and 10-year-old pediatric phantoms based on polygon mesh surfaces. Med. Phys. 38 (8), 4723–4736. https://doi.org/10.1118/1.3615623.

Huda, W., Chamberlain, C., Rosenbaum, A., Garrisi, W., 2001. Radiation doses to infants and adults undergoing head CT examinations. Med. Phys. 28 (3), 393–399. https://doi.org/10.1118/1.1350435.

ICRP Publication 116. Conversion Coefficients for Radiological Protection Quantities for External Radiation Exposures, Ann. ICRP 40 (2–5), 2010.

Meyer, P., Buffard, E., Mertz, L., Kennel, C., Constantinesco, A., Siffert, P., 2004. Evaluation of the use of six diagnostic x-ray spectra computer codes. Br. J. Radiol. 77 (915), 224–230(pMID: 15020364. URL ⟨https://doi.org/10.1259/bjr/32409995⟩).

Mohammadi, G.F., Alam, N.R., Geraily, G., Paydar, R., 2016. Thorax organ dose estimation in computed tomography based on patient ct data using monte carlo simulation. Int. J. Radiat. Res. 14 (4). https://doi.org/10.18869/acadpub.ijrr.14.4.313. arXiv:http://ijrr.com/article-1-1816-en.pdf. http://ijrr.com/article-1-1816-en.html.

Pelowitz, D.B., 2011. MCNPX User's Manual, Version 2.7.0, Report LA-CP-11-00438. Los Alamos National Laboratory.

Spampinato, M., Tipnis, S., Tavernier, J., Huda, W., 2015. Thyroid doses and risk to paediatric patients undergoing neck ct examinations. Eur. Radiol. 25 (7), 1883–1890. https://doi.org/10.1007/s00330-015-3590-x.

Vieira, J.W., Lima, F.R.A., 2009. A software to digital image processing to be used in the voxel phantom development. Cell. Mol. Biol. 55 (3), 16–22.

Yang, C.C., Liu, S.H., Mok, G.S., Wu, T.H., 2014. Evaluation of radiation dose and image quality of CT scan for whole-body pediatric PET/CT: a phantom study. Med. Phys. 41 (9), 092505. https://doi.org/10.1118/1.4893273.